Universiteit Leiden
The Netherlands

The endothelial glycocalyx in diabetic nephropathy and beyond

Boels, M.G.S.

Citation
Boels, M. G. S. (2018, September 6). *The endothelial glycocalyx in diabetic nephropathy and beyond*. Retrieved from https://hdl.handle.net/1887/64937

Version:	Not Applicable (or Unknown)
License:	Licence agreement concerning inclusion of doctoral thesis in the Institutional Repository of the University of Leiden
Downloaded from:	https://hdl.handle.net/1887/64937

Note: To cite this publication please use the final published version (if applicable).

Cover Page

Universiteit Leiden

Leiden University Repository

The handle http://hdl.handle.net/1887/64937 holds various files of this Leiden University dissertation.

Author: Boels, M.G.S.
Title: The endothelial glycocalyx in diabetic nephropathy and beyond
Issue Date: 2018-09-06

Chapter 5

Endothelial glycocalyx remodeling by heparanase induces endothelial dysfunction

Margien G.S. Boels, Gangqi Wang, Wendy M.P.J. Sol, Annemarie M.A. de Graaf, Toine van Kuppevelt, Johan van der Vlag, Hermann Haller, Bernard M. van den Berg, Ton J. Rabelink

Abstract

Heparan sulfate chains are important constituents of the endothelial glycocalyx where they regulate the activity of numerous bioactive molecules such as cytokines and growth factors at the cell surface. Heparanase is an endo-b-glucuronidase that hydrolyzes glucuronic acid–*N*-acetylglucosamine linkages in heparan sulfate chains. Its synthesis and release is induced upon inflammation and during metabolic stress, and can be activated in the extracellular space by L cathepsin. We postulate that extracellular heparanase activity serves to adapt the endothelial surface to inflammation. While prolonged laminar shear stress is shown in our study to be associated with robust heparan sulfate synthesis and a quiescent phenotype in a microfluidic culture system, increasing luminal heparanase activity is not only accompanied by a reduction in endothelial surface glycocalyx, but also by increased expression of inflammatory heparan sulfate epitopes. In addition, endothelial gene expression of inflammatory cytokines is increased as well. To extend these observations to the *in vivo* situation, active heparanase was perfused in zebrafish larvae, where a similar change in inflammatory heparan sulfate domains was observed in the vasculature. We conclude that activation of heparanase at the endothelial surface, serves remodeling of the endothelial glycocalyx to support inflammatory processes.

Introduction

Heparanase is the only known mammalian endoglycosidase capable of enzymatic degradation of heparan sulfates (HS). Heparanase is involved in intracellular processes such as gene transcription and autophagy (1). However, in situations such as diabetes (2) and other inflammatory diseases (3), heparanase can be released to and activated in the extracellular matrix were it can degrade HS. HS is an important constituent of the endothelial glycocalyx, a delicate layer of interconnected carbohydrates, which is critical for endothelial function. Bound to proteins such as syndecans, glypican and versican, HS forms proteoglycans (4). In the Golgi apparatus, were HS is produced and attached to a core protein, extensive modification of HS occurs. The sulfation pattern of HS is responsible for highly specific binding of proteins at the endothelial surface (5,6). For example, the binding of various growth factors, such as fibroblast growth factor 2 (FGF-2) or vascular endothelial growth factor (VEGF), and cytokines critically depends on binding to a specifically HS moieties (7-9). In addition, HS within the extracellular matrix can via these modifications generate chemokine gradients over the endothelium to guide cells towards the underlying tissue (10). Since HS are made up of up to 150 modifiable disaccharide units there is a high variety in binding sites for different proteins (5,7,11). Consequently, HS are involved in a variety of processes such as cell attachment, migration, differentiation, blood coagulation, lipid metabolism, and inflammation (4,12-14). Because the production of HS is continuously ongoing and availability of enzymes and substrates can vary, the sulfation pattern can be rapidly modified and adjusted to changing environments (15,16). Next to the intracellular enzymes that are responsible for HS make-up, extracellular HS can be degraded by heparanase, an endo-beta-glucuronidase that cleaves/hydrolyzes HS chains at GlcA(b1→4) GlcNAc linkages into fragments of 10-20 sugar units (17).

In the current study we postulate that degradation of HS in the endothelial glycocalyx by heparanase facilitates glycocalyx turnover, and adaptation to inflammation and metabolic stress. To this end, we used a panel of glycoprobes against specific domains within the HS structures of the endothelial glycocalyx, in the absence and presence of active heparanase. Where the 10E4 antibody recognizes so-called mixed HS domains, containing both N-acetylated and N-sulfated disaccharide units, JM403 recognizes more N-unsubstituted glucosamine residues (18). Furthermore, single chain antibodies were used to map smaller HS domains, with more specific binding properties. For example, the N-, and 6-O-sulfated domains that are recognized by AO4B08 play a role in growth factor binding (19), such as VEGF and FGF, and are highly expressed in certain tumor cells (20). Using such variety of glycoprobes and single chain antibodies, we show that heparanase not only reduces total surface glycocalyx coverage but also changes the composition of HS binding domains to support inflammatory mediators.

Materials and Methods

Shear stress experiments

HUVEC were isolated from umbilical cords by perfusion and subsequent 20 minutes incubation of trypsin at 37°C. Freshly isolated HUVECs were cultured on 0.5% gelatin coated plastic flasks in EGM2 medium (Lonza, Basel, Switzerland) supplemented with antibiotics/antimycotics (Life technology, Gibco) and were used for experiments at passage 1-3. HUVECs were seeded into closed perfusion chambers (ibiTreat µ-Slide VI 0.4 Luer and µ-Slide I 0.4 Luer, Ibidi GmbH, Marensried, Germany) at a concentration of $1.5*10^6$ cells per mL. After cells were allowed to adhere for 3 hours, the chamber was connected to a computer-controlled air pressure pump and a fluidic unit with a two-way switching valve (Ibidi). The pump setup allowed pumping of 16 mL cell culture medium from two reservoirs in a unidirectional way through the flow channel over the monolayer of endothelial cells at a constant shear stress of 10 dyne/cm^2. Medium was refreshed after 1 day, to remove non-adhered cells, and continued with 4 days of culture. A subset of cells was exposed to active recombinant heparanase (100 ng/mL, R&D Systems Europe Ltd, Abingdon, UK) for the last 24 hours. The chamber and the reservoirs containing the medium were kept in an incubator at 37°C and 5% CO_2. For static control experiments, cells were cultured in perfusion chambers, not attached to an air pressure pump.

Cell culture and confocal immunofluorescence microscopy

After static culture (24 hours) or exposure to flow (1, 4 or 7 days) in a µ-Slide VI 0.4 Luer flow chamber (6 lanes), HUVECs were fixed in freshly made 4% paraformaldehyde for 10 minutes, washed twice with HBSS (life technologies) and blocked for 30 minutes with 3% normal goat serum (NGS) in HBSS. Cells were incubated overnight at 4°C with one of the primary antibodies (at 10 µg/mL): 10E4 (Amsbio), JM403 (kind gift of Dr. van der Vlag, Radboud University Medical Centre, Nijmegen, The Netherlands), the single chain antibodies EW4G2, AO4B08 and HS4C3 (kind gift of Dr. van Kuppevelt, Radboud University Medical Centre Nijmegen, The Netherlands), CS56 against chondroitin sulfate (Abcam, Cambridge, MA), VE-cadherin (BD biosciences, San Jose, CA), phalloidin-rhodamine (Sigma-Aldrich), or the appropriate control IgM or IgG isotype antibodies diluted in HBSS. After washing three times with HBSS, cells were incubated with a secondary antibody for 1 hour (anti-mouse IgM-Alexa488; anti-mouse IgG-Alexa488 or anti-VSV-DyLight488) and Hoechst 33528 (1/1,000, Sigma-Aldrich, St. Louis, MO), followed by tetramethylrhodamine-labeled wheat germ agglutinin (WGA) (1/100; Sigma-Aldrich) for 30 min. Cells were again washed for three times with HBSS and imaged using a confocal microscopy at 63x objective.

CLSM image analysis and quantification

Confocal 12-bit gray-scale axial image stacks (xyz dimensions, 0.08×0.08×0.13 µm) that covered 6724 μm^2 of surface area per image and a height of 5 to 10 µm above the EC nuclear plane were recorded using Leica Application Suite Advanced Fluorescence image software

(Leica) to create image stacks. The image stacks were analyzed with the public domain National Institutes of Health IMAGE program (available at http://rsb.info.nih.gov/nih-image). For luminal endothelial glycocalyx thickness quantification, first nuclear and peri-nuclear area was selected, to exclude the cell area in which the cell thickness was too thin to differentiate between luminal and abluminal staining. Thickness of the lectin (WGA and LEA) stained layer was estimated within this area of interest, between the half-maximum nuclear (Hoechst) signal and the luminal half-maximum of lectin fluorescence. Total luminal signal distribution and heterogeneity of specific HS sequences were calculated in the same 3-dimensional area of interest in every z-plane within this area (area%). A visualization of this method is shown in supplementary figure S1.

RNA Isolation and RT-qPCR

After static culture (24 hours) or exposure to flow (24 hours or 7 days) in a μ-Slide I 0.4 Luer flow chamber (1 lane), total RNA was isolated from HUVECs cultured in a μ-Slide I 0.4 using Trizol reagent (Life Technologies) and isolation kit (Qiagen). Reverse transcription was performed after a 5-minute 65°C incubation of 500 ng total RNA with deoxyribonucleotide triphosphates (Life Technologies) and oligo(dT) (Life Technologies): cDNA was synthesized using M-MLV First-Strand Synthesis (Life Technologies), and validation was carried out using SYBR Green Master Mix (Life technologies). Levels of expression were determined by normalizing to GAPDH levels.

Zebrafish larvae

Transgenic Tg(l-fabp:DBP-eGFP) zebrafish larvae were grown and mated at 28.5°C (21). Embryos were kept and handled in standard E3 solution (5mM NaCl, 0.17 mM KCl, 0.33 mM CaCl2, 0.33 mM MgSO4, 10^{-5}% methylene blue) buffered with 2 mM HEPES (Sigma-Aldrich, St. Louis, MO). All zebrafish larvae studies were conducted in accordance with the National Institutes of Health (NIH) Guide for the Care and Use of Laboratory Animals. Using the Nanoject II injection device (Drummond Scientific, Broomall, PA), 5 nL heparanase (0.15 mg/mL, Amsbio) or control solution (PBS) was injected into zebrafish larvae 72 hours post fertilization (hpf). After 24 hours (4 days post fertilization (dpf)), glomerular function was measured, as described previously (21). These zebrafish larvae express a GFP-tagged vitamin D binding protein with a molecular weight of 78 kDa under the control of the l-fabp (liver-type fatty acid binding protein promotor), therefore diminished fluorescence in the vasculature indicates accelerated protein leakage though the pronephros. Zebrafish larvae were anesthetized with a 1:20 to 1:100 dilution of 4 mg/ml Tricaine (MESAB: ethyl-3-aminobenzoate, methanesulfonate acid salt, 1% Na2HPO4, pH 7.0) (Sigma-Aldrich). Pupils of the zebrafish larvae were imaged using a Zeiss inverted microscope (Axiovert 200) connected to an AxioCam MRm charge-coupled device camera. Images were taken with fixed exposure times and gain using the Axio Vision release 4.5 SP1 software package to quantify maximum fluorescence intensity. Subsequently, zebrafish larvae were sampled and fixed in 4% PFA for 24 hours. After fixation, the zebrafish

larvae were incubated for 24 hours with 30% sucrose, embedded in Tissue-Tek O.C.T. (Sakura Finetek, Alphen aan den Rijn, The Netherlands) and cryopreserved a -80°C. Sections of 10 µm were permeabilized with 0.3% Triton-X100 and stained as described above for HUVECs and were image with Leica DMI6000 and confocal microscopy for blinded quantification of staining intensity (percentage of stained area divided by the total area in ImageJ).

Statistical analyses

Data are presented as mean ± SEM obtained from four to six independent experiments (n = 4-6), unless indicated otherwise. All *in vitro* and *in vivo* results were analyzed using GraphPad software version 5.0 (GraphPad Prism Software Inc, San Diego, CA) with either a *t* test or analysis of variance (using a Bonferonni post-hoc test). Differences in P-values < 0.05 were considered statistically significant.

Results

Prolonged laminar shear stress induces quiescent endothelial phenotype

To confirm earlier reports on the effect of shear stress to endothelial cells (22-24) we analyzed cell morphology and expression of shear responsive genes and proteins. After 4 - 7 days of a laminar shear stress of 10 dyne/cm^2 HUVECs aligned into the direction of flow with increased expression of VE-cadherin at the cell borders and typical short F-actin shear fibers, in comparison to static cultures (Figure 1A). In addition, shear stress sensitive genes Krüppel-like Factor 2 (KLF2) and endothelial nitric oxide synthase (eNOS) were upregulated. In contrast, gene expression of the inflammatory markers E-selectin and IL-8 were decreased (Figure 1B). In line with previous data (25), IL-8 gene expression was highly increased after 24 hours of exposure to shear stress, which confirms an acute inflammatory response upon exposure to shear stress. However, IL-8 expression returned to base-line levels after 4 days of flow. In addition, superoxide dismutase-1 (SOD1) gene expression, which in the presence of catalase keeps intracellular oxidant levels low (26), is upregulated after 4 days of flow. In short, shear stress initially provokes an inflammatory cascade in endothelial cells, whereas prolonged shear stress induces a quiescent phenotype.

Prolonged laminar shear stress increases glycocalyx thickness

We tested the time necessary for endothelial cells to express a sufficient luminal glycocalyx. For this, we stained the glycocalyx after indicated time periods with the *N*-acetylneuraminic acid and *N*-acetyl-β-D-glucosamine binding lectin from *Triticum vulgaris* ((WGA), Figure 1C). Four days of exposure to 10 dyne/cm^2 shear stress induces a maximum total intensity of luminal WGA staining and was significantly ($p < 0.05$) increased in thickness in comparison to static and 1 day of flow (Figure 1D). Thickness remained equally high up to 7 days of flow. To determine whether the composition of HS within the endothelial glycocalyx could be affected by changes

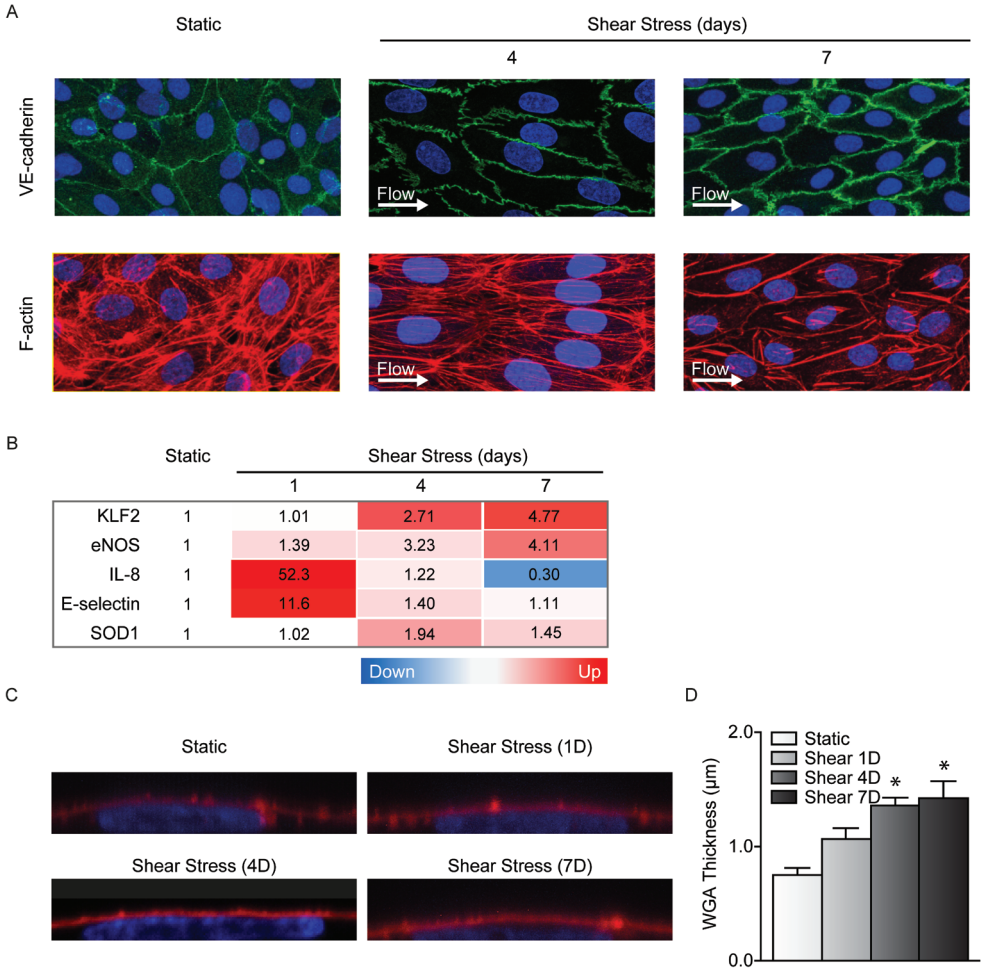

Figure 1. Prolonged shear stress induces quiescent endothelium. A) Cell morphology changes upon prolonged shear stress culture. HUVEC are stained with antibodies against VE-cadherin (upper) and the F-actin binding phalloidin-rhodamine (lower) to visualize endothelial phenotypic changes. Static cultured HUVEC (left) were compared to HUVEC cultured for 4 days (middle) and 7 days (right) at a shear stress of 10 dyne/cm^2. B) Relative expression of selected genes for endothelial function that show response to shear stress of 1, 4 or 7 days (fold change compared to static culture): Krüppel-like Factor 2 (KLF2), endothelial nitric oxide synthase (eNOS), Interleukine-8 (IL-8), E-selectin and Superoxide dismutase-1 (SOD1). C) Representative examples of wheat germ agglutinin (WGA) staining on top of the endothelial cells after 24 hours of static culture or exposure to shear stress for 1, 4 or 7 days (D). D) Quantification of luminal WGA staining relative to static culture (quantification method described in figure S1), expressed as mean ± SD of 4-5 independent experiments; *$p < 0.05$ compared to static and shear for 1 day.

in gene expression upon shear stress, gene expression levels of key enzymes involved in HS polymerizing and sulfation pattern modification were studied. Four days of flow exposure increases the HS polymerase enzymes exostosin 1 and 2 (EXT1 and EXT2), as well as the first enzyme in HS modification, N-deacetylase/Nsulfotransferase-1 (NDST1; Supplementary Figure S2A). Whereas, the intracellular HS chain modifying HS sulfotransferases (HS2ST1, HS3ST1 and

HS6ST1) were variably changed upon shear stress stimulation. In addition, the extracellular modifying enzymes 6-O-endosulfatase 1 and 2 (SULF1, SULF2) and heparanase (HPSE1) were all increased upon four days of shear stress.

Extracellular heparanase modifies the endothelial glycocalyx

To test the effect of extracellular heparanase on the endothelial glycocalyx we incubated endothelial cells with active heparanase during the last 24 hours of the 4-day shear stress experiments. Heparanase decreased total WGA luminal coverage ($p < 0.05$, data not shown). We further tested possible compositional changes using various antibodies against specific domains on the HS chain. For this purpose, we tested the two IgM-type antibodies 10E4 and JM403, and the three single chain antibodies EW4G2, AO4B08 and HS4C3 (27,28), with the specific domains recognized shown in Figure 2A. Quantification of luminal antibody staining was performed in the same area as described above (Supplementary Figure S1). After 4 days of flow exposure, luminal expression of 10E4 was most abundant (12.8 ± 6.5%), followed by JM403 (8.5 ± 3.7%), (Figure 2B and C). The expression levels of the single chain antibodies after 4 days of shear stress was highest for EW4G2 (2.5 ± 1.5%) while AO4B08 (0.2 ± 0.3%) and HS4C3 (0.6 ± 1.1%) expression levels were very low. Incubation with heparanase dramatically decreased both the presence of 10E4 and JM403 binding sites on the luminal surface (3.4 ± 2.7 and 4.4 ± 2.6%, respectively; $P<0.05$ compared to shear stress alone) Exposure to heparanase only resulted in a significant increase of AO4B08 (1.2 ± 0.7%; $p < 0.05$), while both EW4G2 and HS4C3 revealed only a small, non-significant, elevation.

We included an IgM-type antibody against chondroitin sulfate (CS56) to examine whether a reduction in HS induces compensatory chondroitin sulfate biosynthesis (29). While the expression level of chondroitin sulfate was very low in standard 4-day shear stress culture (1.5 ± 0.3%), heparanase treatment induces chondroitin sulfate to 4.3 ± 1.5% ($p < 0.05$).

Extracellular heparanase stimulates the expression of inflammatory genes in endothelial cells

Although heparanase was given extracellularly, glycocalyx degradation or direct enzyme uptake might influence the endothelial cell itself. Therefore, we also studied cell morphology and expression of shear responsive genes and proteins after 24 hours heparanase treatment of cells exposed to 4 days of 10 dyne/cm^2 shear stress. While no changes in expression of genes involved in HS biosynthesis and modification were observed (Supplementary Figure S2A), the presence of extracellular heparanase resulted in increased unstable focal adhesion junctions as visualized by VE-cadherin staining, less organized actin filaments, without evident changes in cell orientation in response to flow in comparison to 4 days flow exposure (Supplementary Figure S2B and C). Heparanase treatment resulted also in a reduced KLF2 and eNOS gene expression, while IL8 and E-selectin gene expression were increased (Figure 2D).

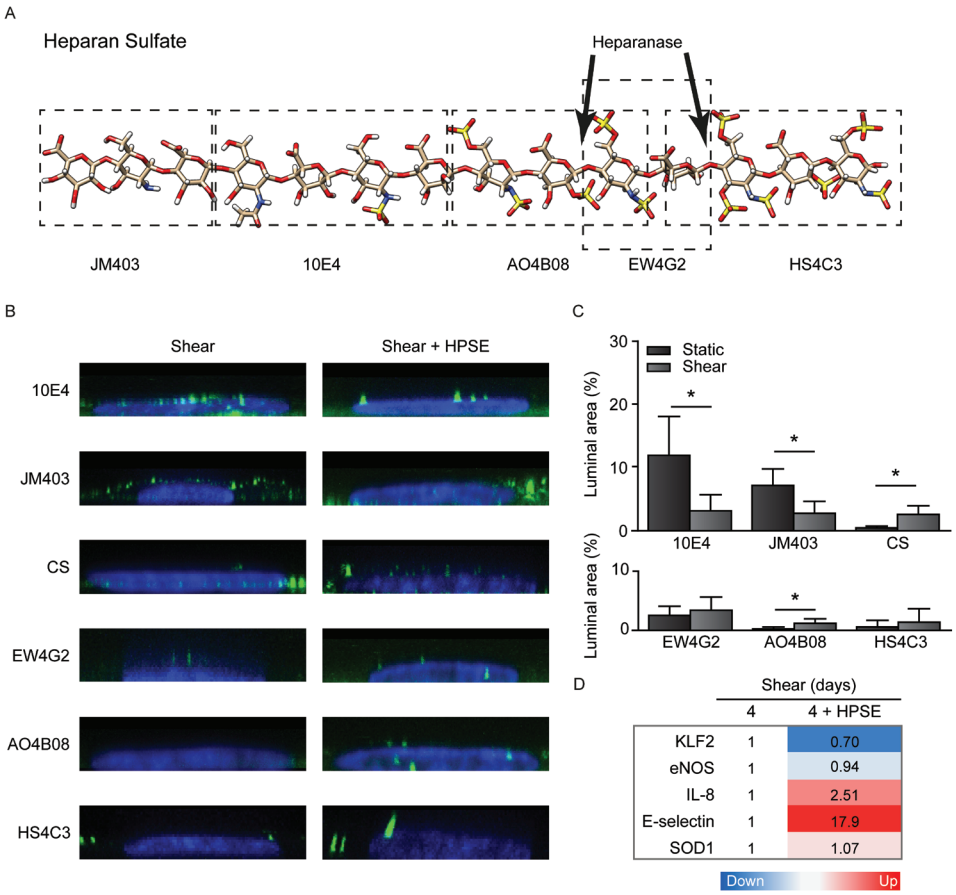

Figure 2. Heparanase changes endothelial glycocalyx in HUVEC cultured under flow. A) Structure model of heparan sulfate showing the tetrasaccharide repeat of glucuronic acid (GlcA) and N-, 6-O-sulfated glucosamine GlcN(NS,6S) in which, as a first step in cleavage, heparanase will cut the following tri-saccharide from the non-reducing end. In the structure the carbon backbone (brown), oxygen (red), hydrogen (white), sulfide (yellow) and nitrogen (blue) are depicted. The binding domains of used antibodies are shown (JM403, 10E4, AO4B08, EW4G2 and HS4C3). B) Representative examples of heparan sulfate specific domains (10E4, JM403, EW4G2, AO4B08 and HS4C3) and Chondroitin Sulfate (CS) staining in HUVEC exposed to shear stress for 4 days ± heparanase. C) Luminal staining area of B is quantified in the same area of interest as in figure S1 and expressed as area percentage ± SD; *$p < 0.05$ E) Expression of selected genes for endothelial glycocalyx stabilization after 4 days of shear stress ± heparanase: Krüppel-like Factor 2 (KLF2), endothelial nitric oxide synthase (eNOS), Interleukine-8 (IL-8), E-selectin and Superoxide dismutase-1 (SOD1). Genes are expressed as fold change compared to 4 days of culture and expressed as mean of 4-5 independent experiments; *$p < 0.05$.

Systemic heparanase changes vascular heparan sulfate composition in zebrafish

To test the effect of extracellular heparanase in the circulation *in vivo*, we injected heparanase in the cardinal vein of zebrafish larvae 3 days post fertilization (dpf). At 4 dpf, 24 hours after systemic heparanase injection, we quantified binding of the various anti-HS antibodies to all

vessels within the cross-sectional area of the pronephros, as shown in Figure 3A and B. Systemic heparanase treatment decreased the binding sites for both 10E4 (13.7 ± 5.8% vs. wild type 20.5 ± 6.2%) and JM403 (27.4 ± 8.0% vs. wildtype: 37.8 ±16.1%; $p < 0.05$; Figure 3B).

In line with the observations in HUVECS, AO4B08 expression was significantly increased upon extracellular heparanase presence (25.6 ± 9.2% vs. control 10.0 ± 8.4%; $p < 0.01$). In addition, the other antibody EW4G2 recognizing the N-, and 6-O-sulfated domains of HS was increased also significantly (10.9 ± 6.6% vs. wild type 1.6 ± 1.6%; $p < 0.01$). Throughout the vasculature analyzed, the typical 3-O-sulfated domains recognized by HS4C3 hardly was expressed in the zebrafish larvae, and not affected by systemic heparanase perfusion (0.8 ± 0.8% vs. wildtype:

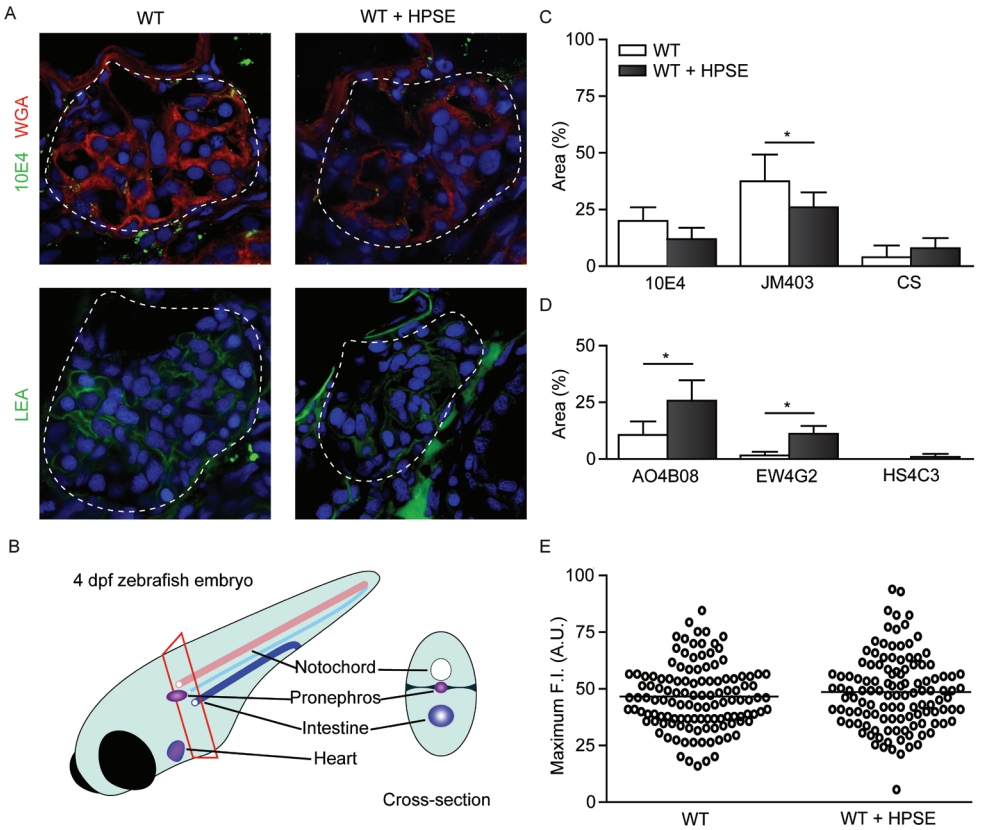

Figure 3. Systemic heparanase changes glycosaminoglycan composition in zebrafish larvae. A) Representative pictures of wheat germ agglutinin (WGA; top), and Lycopersicon esculentum (LEA; bottom) staining in the pronephros (encircled dashed) of zebrafish larvae with or without exposure to systemic heparanase (HPSE). B) schematic representation of zebrafish embryo, 4 days post fertilization (4 dpf; left) with cross-sectional area where quantification in C & D took place (right). C) Staining area of specific heparan sulfate epitopes are expressed as vascular area percentage ± SD; *$p < 0.05$. WT = wild type; WT + HPSE = WT perfused with heparanase for 24 hours; CS = Chondroitin Sulfate. D) Intravascular fluorescence loss is measured over the retinal blood vessel plexus in Tg(l-fabp:DBP-eGFP) fish after control (WT) and heparanase (WT + HPSE) injection at 4 days post fertilization to analyze vascular leakage in zebrafish larvae. Maximum Fluorescence levels (F.I.) of individual zebrafish larvae are displayed.

0.9 ± 1.4%, Figure 3D). Similar as was found in HUVECS, we observed a compensatory increase in chondroitin sulfate from 4.1 ± 2.7% to 9.2 ± 4.1%, Figure 3C).

To analyze the possible consequences of systemic glycocalyx alterations, we measured vascular leakage, as analyzed in the eye of the zebrafish larvae (21). Treatment with heparanase for 24 hours did not change fluorescence (Figure 3E), thus although systemic heparanase modified HS structure, it did not induce overt vascular leakage in these zebrafish larvae.

Discussion

Introducing extracellular active heparanase within the milieu of endothelial cells cultured under prolonged shear stress not only reduces total surface glycocalyx coverage but also changes the composition of HS binding domains to support inflammatory mediators.

Endothelial HS binds chemokines to create a gradient that supports initial leukocyte tethering and directs their migration across the endothelium (14). HS on the glycocalyx surface of inflammatory cells and endothelial cells enables direct physical interaction between the endothelial and inflammatory cells and enables the engagement of cell surface receptors with their ligands such as adhesion molecules (30). The HS constituent of the cell surface layer is very dynamically regulated. For example, rapid changes in sulfation patterns can occur in response to inflammatory stimuli through the upregulation of modifying enzymes such as *NDST-1* in a matter of hours (31). We have demonstrated that such HS modifications are key to the ability of inflammatory cells to invade the glomerulus during glomerulonephritis (27). To enable such rapid remodeling, an equally dynamic method for the degradation of HS components on the cell surface layer is required. HS carrying proteoglycans (HSPGs) and (pro)heparanase are continuously internalized (32). Once processed into its activated form in the endosome, heparanase can be taken up by the Golgi system again where it might remodel HS synthesis (33,34). This recycling of HSPGs and heparanase is hypothesized to contribute to the dynamic regulation of HS on the cell surface and cellular adaptation to processes such as inflammation. Our current studies further corroborate this hypothesis both *in vitro* as well as *in vivo*.

We also show that selective loss of HS structures via heparanase is compensated in part by increased chondroitin sulfate biosynthesis, as has also been described previously (29) This may have allowed preservation of barrier function. Indeed, in zebrafish larvae, the infusion of heparanase did not induce overt vascular leakage. This is most likely related to the fact that we chose our heparanase dosage to mimic concentrations that can be observed during inflammation, where the glycocalyx barrier structure is reduced (as illustrated by the reduction in lectin staining, Figure 3A) but not completely lost.

The relevance of these observations pertains to conditions where heparanase is secreted and subsequently activated in the extracellular space. These conditions include cancer invasion, neoangiogenesis, diabetic nephropathy and glomerulonephritis (35-42). Interestingly, the upregulation of endothelial HS domains by heparanase as was identified by the single chain antibodies AO4B08 and EW4G2 is very similar to what has been previously observed by us in

conditions with endothelial activation such as in glomerulonephritis (27). The potential relevance of heparanase in these conditions, and as a potential therapeutic avenue, is underscored by the fact that genetic deletion of heparanase can prevent the development of glomerulonephritis and diabetic nephropathy (2).

Acknowledgements

The Dutch Kidney Foundation financially supported this study: Glycoren consortium (CP09.03).

We thank L. Staggs, P. Schroder and Dr. S. Rieger (Mount Desert Island Biological Laboratory, Salisbury Cove, ME) for the use of the zebrafish facilities.

References

1. Rabelink TJ, van den Berg BM, Garsen M, Wang G, Elkin M, et al. (2017) Heparanase: roles in cell survival, extracellular matrix remodelling and the development of kidney disease. Nat Rev Nephrol 13: 201-212.
2. Gil N, Goldberg R, Neuman T, Garsen M, Zcharia E, et al. (2012) Heparanase is essential for the development of diabetic nephropathy in mice. Diabetes 61: 208-216.
3. Lever R, Rose MJ, McKenzie EA, Page CP (2014) Heparanase induces inflammatory cell recruitment in vivo by promoting adhesion to vascular endothelium. Am J Physiol Cell Physiol 306: C1184-1190.
4. Reitsma S, Slaaf DW, Vink H, van Zandvoort MA, oude Egbrink MG (2007) The endothelial glycocalyx: composition, functions, and visualization. Pflugers Arch 454: 345-359.
5. Esko JD, Selleck SB (2002) Order out of chaos: assembly of ligand binding sites in heparan sulfate. Annu Rev Biochem 71: 435-471.
6. Rops AL, Jacobs CW, Linssen PC, Boezeman JB, Lensen JF, et al. (2007) Heparan sulfate on activated glomerular endothelial cells and exogenous heparinoids influence the rolling and adhesion of leucocytes. Nephrol Dial Transplant 22: 1070-1077.
7. Esko JD, Lindahl U (2001) Molecular diversity of heparan sulfate. J Clin Invest 108: 169-173.
8. Quarto N, Amalric F (1994) Heparan sulfate proteoglycans as transducers of FGF-2 signalling. J Cell Sci 107 (Pt 11): 3201-3212.
9. Yayon A, Klagsbrun M, Esko JD, Leder P, Ornitz DM (1991) Cell surface, heparin-like molecules are required for binding of basic fibroblast growth factor to its high affinity receptor. Cell 64: 841-848.
10. Massena S, Christoffersson G, Hjertstrom E, Zcharia E, Vlodavsky I, et al. (2010) A chemotactic gradient sequestered on endothelial heparan sulfate induces directional intraluminal crawling of neutrophils. Blood 116: 1924-1931.
11. Lindahl U, Kusche-Gullberg M, Kjellen L (1998) Regulated diversity of heparan sulfate. J Biol Chem 273: 24979-24982.
12. Broekhuizen LN, Mooij HL, Kastelein JJ, Stroes ES, Vink H, et al. (2009) Endothelial glycocalyx as potential diagnostic and therapeutic target in cardiovascular disease. Curr Opin Lipidol 20: 57-62.
13. Lee DH, Dane MJ, van den Berg BM, Boels MG, van Teeffelen JW, et al. (2014) Deeper penetration of erythrocytes into the endothelial glycocalyx is associated with impaired microvascular perfusion. PLoS One 9: e96477.
14. Esko JD, Selleck SB (2002) Order out of chaos: assembly of ligand binding sites in heparan sulfate. Annu Rev Biochem 71: 435-471.
15. Kolset SO, Reinholt FP, Jenssen T (2012) Diabetic nephropathy and extracellular matrix. J Histochem Cytochem 60: 976-986.
16. Uchimura K, Lemjabbar-Alaoui H, van Kuppevelt TH, Rosen SD (2010) Use of a phage display antibody to measure the enzymatic activity of the Sulfs. Methods Enzymol 480: 51-64.
17. Wilson JC, Laloo AE, Singh S, Ferro V (2014) 1H NMR spectroscopic studies establish that heparanase is a retaining glycosidase. Biochem Biophys Res Commun 443: 185-188.
18. van den Born J, Salmivirta K, Henttinen T, Ostman N, Ishimaru T, et al. (2005) Novel heparan sulfate structures revealed by monoclonal antibodies. J Biol Chem 280: 20516-20523.
19. Kreuger J, Spillmann D, Li JP, Lindahl U (2006) Interactions between heparan sulfate and proteins: the concept of specificity. J Cell Biol 174: 323-327.
20. Ferreras C, Rushton G, Cole CL, Babur M, Telfer BA, et al. (2012) Endothelial heparan sulfate 6-O-sulfation levels regulate angiogenic responses of endothelial cells to fibroblast growth factor 2 and vascular endothelial growth factor. J Biol Chem 287: 36132-36146.
21. Kirsch T, Kaufeld J, Korstanje R, Hentschel DM, Staggs L, et al. (2013) Knockdown of the hypertension-associated gene NOSTRIN alters glomerular barrier function in zebrafish (Danio rerio). Hypertension 62: 726-730.
22. Dekker RJ, van Soest S, Fontijn RD, Salamanca S, de Groot PG, et al. (2002) Prolonged fluid shear stress induces a distinct set of endothelial cell genes, most specifically lung Kruppel-like factor (KLF2). Blood 100: 1689-1698.

23. Boon RA, Leyen TA, Fontijn RD, Fledderus JO, Baggen JM, et al. (2010) KLF2-induced actin shear fibers control both alignment to flow and JNK signaling in vascular endothelium. Blood 115: 2533-2542.
24. Dane MJC (2015) Structure and function of the endothelial glycocalyx in the microcirculation. (dissertation). Chapter 3, Prolonged shear stress modifies the composition of the endothelial glycocalyx; p. 50-67. Leiden: Leiden University Medical Center. 50-67 p.
25. Boon RA, Horrevoets AJ (2009) Key transcriptional regulators of the vasoprotective effects of shear stress. Hamostaseologie 29: 39-40, 41-33.
26. Grobe AC, Wells SM, Benavidez E, Oishi P, Azakie A, et al. (2006) Increased oxidative stress in lambs with increased pulmonary blood flow and pulmonary hypertension: role of NADPH oxidase and endothelial NO synthase. Am J Physiol Lung Cell Mol Physiol 290: L1069-1077.
27. Rops ALWM, Loeven MA, van Gemst JJ, Eversen I, Van Wijk XM, et al. (2014) Modulation of heparan sulfate in the glomerular endothelial glycocalyx decreases leukocyte influx during experimental glomerulonephritis. Kidney Int 86: 932-942.
28. Rops AL, van den Hoven MJ, Baselmans MM, Lensen JF, Wijnhoven TJ, et al. (2008) Heparan sulfate domains on cultured activated glomerular endothelial cells mediate leukocyte trafficking. Kidney Int 73: 52-62.
29. Le Jan S, Hayashi M, Kasza Z, Eriksson I, Bishop JR, et al. (2012) Functional overlap between chondroitin and heparan sulfate proteoglycans during VEGF-induced sprouting angiogenesis. Arterioscler Thromb Vasc Biol 32: 1255-1263.
30. Parish CR (2006) The role of heparan sulphate in inflammation. Nat Rev Immunol 6: 633-643.
31. Carter NM, Ali S, Kirby JA (2003) Endothelial inflammation: the role of differential expression of N-deacetylase/N-sulphotransferase enzymes in alteration of the immunological properties of heparan sulphate. J Cell Sci 116: 3591-3600.
32. Yanagishita M, Hascall VC (1992) Cell surface heparan sulfate proteoglycans. J Biol Chem 267: 9451-9454.
33. Roucourt B, Meeussen S, Bao J, Zimmermann P, David G (2015) Heparanase activates the syndecan-syntenin-ALIX exosome pathway. Cell Res 25: 412-428.
34. Nadanaka S, Purunomo E, Takeda N, Tamura J, Kitagawa H (2014) Heparan sulfate containing unsubstituted glucosamine residues: biosynthesis and heparanase-inhibitory activity. J Biol Chem 289: 15231-15243.
35. Escobar Galvis ML, Jia J, Zhang X, Jastrebova N, Spillmann D, et al. (2007) Transgenic or tumor-induced expression of heparanase upregulates sulfation of heparan sulfate. Nat Chem Biol 3: 773-778.
36. van den Born J, van den Heuvel LP, Bakker MA, Veerkamp JH, Assmann KJ, et al. (1993) Distribution of GBM heparan sulfate proteoglycan core protein and side chains in human glomerular diseases. Kidney Int 43: 454-463.
37. van den Hoven MJ, Rops AL, Vlodavsky I, Levidiotis V, Berden JH, et al. (2007) Heparanase in glomerular diseases. Kidney Int 72: 543-548.
38. Katz A, Van-Dijk DJ, Aingorn H, Erman A, Davies M, et al. (2002) Involvement of human heparanase in the pathogenesis of diabetic nephropathy. Isr Med Assoc J 4: 996-1002.
39. Maxhimer JB, Somenek M, Rao G, Pesce CE, Baldwin D, Jr., et al. (2005) Heparanase-1 gene expression and regulation by high glucose in renal epithelial cells: a potential role in the pathogenesis of proteinuria in diabetic patients. Diabetes 54: 2172-2178.
40. Shafat I, Zcharia E, Nisman B, Nadir Y, Nakhoul F, et al. (2006) An ELISA method for the detection and quantification of human heparanase. Biochem Biophys Res Commun 341: 958-963.
41. van den Hoven MJ, Rops AL, Bakker MA, Aten J, Rutjes N, et al. (2006) Increased expression of heparanase in overt diabetic nephropathy. Kidney Int 70: 2100-2108.
42. Wijnhoven TJ, van den Hoven MJ, Ding H, van Kuppevelt TH, van der Vlag J, et al. (2008) Heparanase induces a differential loss of heparan sulphate domains in overt diabetic nephropathy. Diabetologia 51: 372-382.

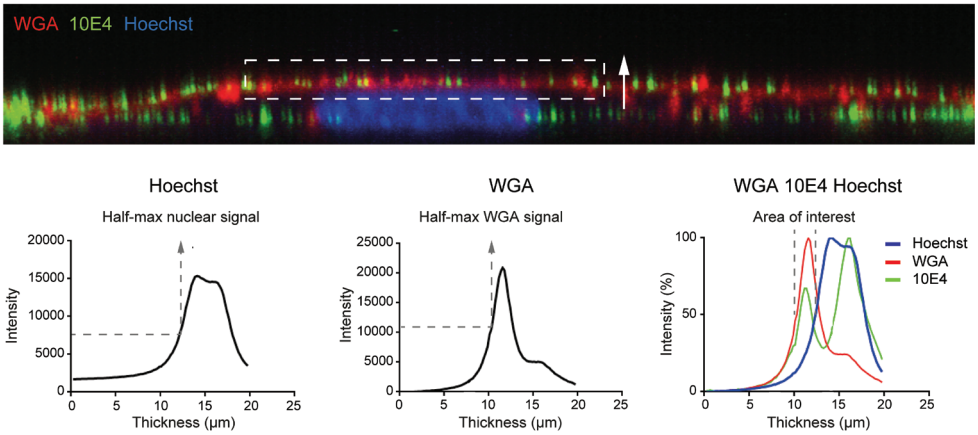

Supplementary Figure S1 Methods to quantify the luminal endothelial glycocalyx staining. A) Confocal fluorescent z-axis average-intensity projections of HUVEC cultured under laminar flow for 4 days and stained with wheat germ agglutinin (WGA), 10E4 and Hoechst. White box shows the area of interest which should be quantified. B) Example of quantification method. Glycocalyx thickness is quantified by estimating the distance from the half-maximum signal of the nuclear staining (left) to the half-maximum signal at the luminal end of WGA (middle) and 10E4 staining (right). Luminal staining area is quantified in the same area of interest in ImageJ.

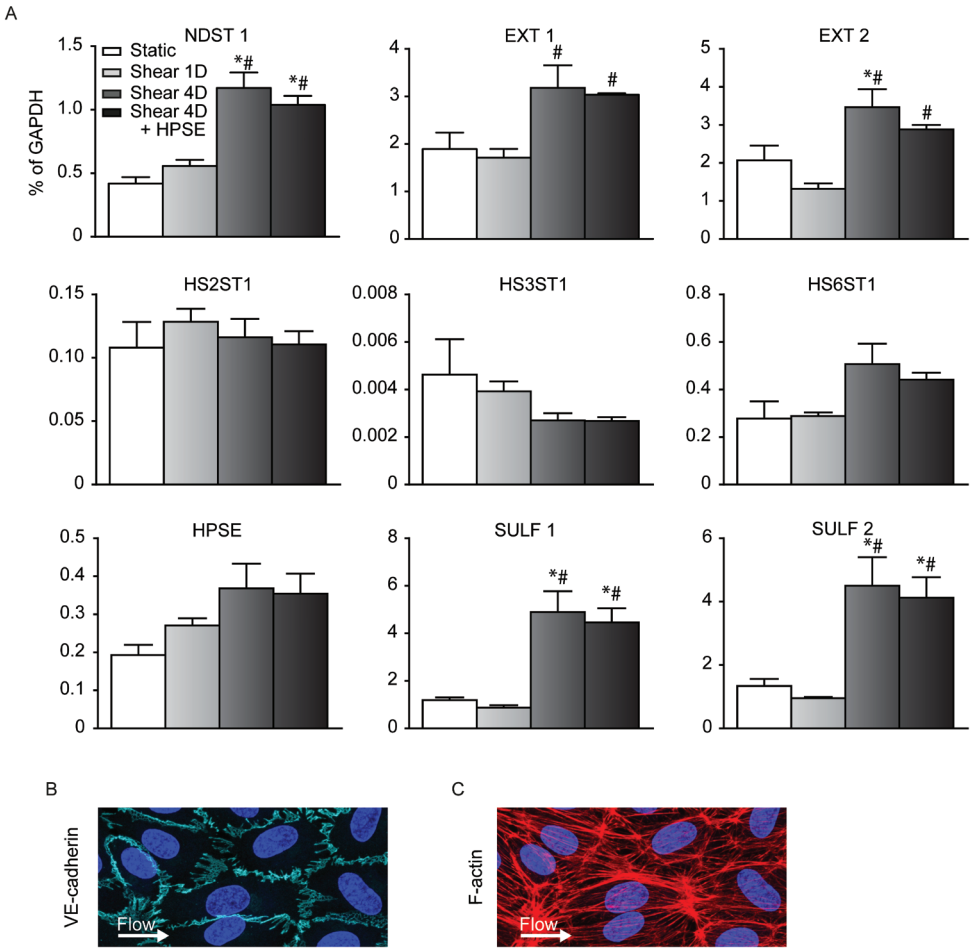

Supplementary Figure S2 Effects of prolonged shear stress on gene expression enzymes involved in HS production and modification. A) Gene expressions as percentage of GAPDH expression after static and 1 or 4 days (D) of flow and 4 days of flow + heparanase (HPSE). Genes coding for enzymes involved in HS chain prolongation (EXT1, EXT2) and sulfation pattern modification (NDST1, HS2ST1, HS3ST1, HS6ST1, SULF1, SULF2) and breakdown (HPSE). Extracellular heparanase induces unstable focal adhesion junctions as visualized by VE-cadherin staining (B) and less organized actin filaments (C), without evident changes in cell orientation in response to flow in comparison to 4 days flow exposure without heparanase. *P<0.05 compared to static culture, #P<0.05 compared to 1day shear stress.